

Spatial Modeling of Earthquake Risk in Sulawesi and Maluku Based on Geological Factors

Syarifah Dey Rahmawati^{1*}

¹Department of Statistics, Faculty of Science and Mathematics, Diponegoro University, Semarang, 50275, Indonesia

* Corresponding author, email: svarifahdesv28@gmail.com

Abstract

The convergence of the Eurasian, Indo-Australian, and Pacific tectonic plates in the Sulawesi and Maluku regions results in high seismic activity, making these areas prone to frequent earthquakes. This study aims to analyze the spatial distribution of earthquake events and assess the influence of geological features such as volcanoes, active faults, and subduction zones on earthquake risk. Using the inhomogeneous Thomas cluster process, spatial modeling was conducted based on earthquake epicenter data from 2009 to 2020 with magnitudes ≥ 4.5 . Each epicenter's distance to the nearest geological feature was used as a covariate. The results of the Chi-square test indicate significant spatial inhomogeneity, while the inhomogeneous K-function reveals that earthquakes tend to occur in clustered patterns. Parameter estimates show that proximity to volcanoes has the most substantial impact, increasing earthquake intensity by approximately 1.8 times for every 100 km closer to a volcano. Faults and subduction zones contribute with relative effects of 0.7 and 0.9 times, respectively. The model demonstrates good fit based on envelope simulation. Earthquake risk prediction maps identify Gorontalo, North Sulawesi, Central Sulawesi, Maluku, and North Maluku as high-risk zones. This model can serve as a valuable tool to support disaster mitigation planning and improve regional earthquake preparedness strategies.

Keywords: Earthquake, Thomas Cluster Process, Spatial Point Process, Sulawesi, Maluku.

1. Introduction

Geographically, Indonesia is located at the convergence of three active tectonic plates: the Eurasian Plate, the Indo-Australian Plate, and the Pacific Plate [1-3]. This convergence leads to frequent seismic activity across the country. Over the past eleven years, the average number of tectonic earthquakes in Indonesia has reached approximately 6,512 events annually [4].

One of the most geologically active regions in terms of time, structure, and tectonics is Sulawesi and its surrounding areas [5]. The convergence of the three plates in the Neogene period triggered the formation of subduction zones, faults, and thrusts across various geological structures and scales. The North Sulawesi subduction zone, Gorontalo fault, Sulu thrust, and Maluku structures are still tectonically active.

The high level of tectonic activity results in frequent earthquakes in Sulawesi and Maluku, often leading to significant casualties. According to the Center for Volcanology and Geological Hazard Mitigation, twelve major earthquakes occurred in Indonesia between 2009 and 2018. One notable event was the 7.6 magnitude earthquake in Palu,

which impacted Palu-Donggala-Sigi-Parigi Moutong, resulting in 7,764 victims, including 4,612 injured, 2,113 deaths, and 1,039 missing persons [6].

One strategy for disaster risk mitigation is modeling earthquake risk using spatial point process methods. A spatial point process is a statistical model that represents patterns of events in d -dimensional space, where each point corresponds to a specific location [7]. These spatial points may represent various phenomena, such as earthquake events, star constellations, traffic accidents, or COVID-19 cases, making it a powerful tool for location-based analysis [8].

Spatial point process methods have previously been applied to evaluate the distribution of gas stations (SPBU) in Surabaya, using the spatial Poisson point process model due to the Poisson-like distribution of the data. The results revealed a non-homogeneous pattern, providing valuable insights for planning the expansion of gas station networks in Surabaya [9].

Another application examined the relationship between modern markets and traditional convenience stores in Surabaya. The model, built using coordinate data from Google Maps, showed that the presence of modern markets influenced the distribution of traditional stores, and that an increase in minimarket density could raise the probability of nearby traditional shops. This suggests that modern markets may stimulate competition rather than eliminate traditional retailers [10].

Previous research by [11] employed the inhomogeneous Thomas cluster process to model the spatial distribution of COVID-19 cases in Greater Surabaya, yielding satisfactory model performance. Other relevant studies on spatial point process modeling have been conducted as well [12-15].

These studies demonstrate that spatial point process methods are effective for modeling coordinate-based phenomena. Given the high seismic activity in the Maluku and Sulawesi regions, it is crucial to perform risk prediction for earthquake occurrences. Therefore, this study aims to predict earthquake risk in the Maluku and Sulawesi Islands using a spatial point process approach. Specifically, the inhomogeneous Thomas cluster process is employed, with covariates including the coordinates of subduction zones, active faults, and volcanoes.

2. Material and Method

The statistical model commonly applied to analyze the distribution pattern of locations such as earthquake epicenters, trees, disease cases, and other spatially random events is the spatial point process. Given that the object of study involves geographical areas, spatial effects or correlations are unavoidable [8]. Depending on the distribution characteristics, spatial correlation patterns are generally classified into three types: cluster, random, and regular [11].

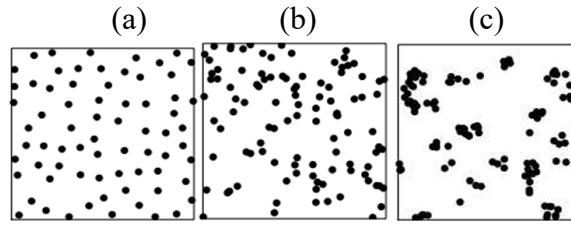


Figure 1. Basic Pattern (a). Regular, (b). Random, (c). Cluster

As shown in Figure 1(a), the regular pattern is characterized by evenly spaced points. In contrast, Figure 1(b) depicts a random scattering of points, while Figure 1(c) illustrates a clustered pattern in which points tend to group together. Mother process (\mathbf{C}) is a key component of the Thomas cluster process, a Poisson process with intensity κ . Around each mother point, an offspring process is generated, described by the following function:

$$\rho_c(\mathbf{u}; \beta) = \exp(\zeta + \beta^T z(\mathbf{u}))k(\mathbf{u} - \mathbf{c}; \omega) \quad (1)$$

$k(\mathbf{u})$ represents the probability density function (PDF) of the distance between offspring and their corresponding mother point \mathbf{C} , parameterized by ω . In the context of seismic analysis, the mainshock serves as the *mother point*, while aftershocks are considered *offspring points*. The PDF for the *Thomas cluster process* is expressed as follows [7]:

$$k(\mathbf{u}) = (2\pi\omega^2)^{-1} \exp(-\|\mathbf{u}\|^2 / (2\omega^2)) \quad (2)$$

The offspring distribution in the Thomas cluster model is independent and follows a bivariate normal distribution $N(0, \omega^2 \mathbf{I})$ [16]. A smaller ω results in more tightly grouped clusters, while a smaller leads to number of parents [11]. The overall intensity function of the process can also be written as:

$$\rho(\mathbf{u}, \beta) = \kappa \exp(\beta^T z(\mathbf{u})) \quad (3)$$

To evaluate spatial dependence among points, the K-function is used. For the Thomas process, it is defined as:

$$K(r) = \pi r^2 + \frac{1}{\kappa} \left(1 - \exp\left(-\frac{r^2}{4\omega^2}\right) \right) \quad (4)$$

To assess whether the observed spatial pattern is homogeneous or heterogeneous, the chi-square test is applied [17]. The first step is dividing the observation window into quadrat, and calculating the number of points within each quadrat: n_1, n_2, \dots, n_m . The hypotheses for the chi-square test are formulated as:

$$H_0: \rho(\mathbf{u}) = \rho(\mathbf{v}); \mathbf{u}, \mathbf{v} \in B \text{ (event intensity is homogeneous)}$$

$$H_1: \rho(\mathbf{u}) \neq \rho(\mathbf{v}); \mathbf{u}, \mathbf{v} \in B \text{ (event intensity is heterogeneous)}$$

The chi-square test statistic is:

$$X_{hitung}^2 = \sum_{j=1}^m \frac{n_j - e_j}{e_j} \quad (5)$$

where:

e_j : number of points in quadrat count to- j

e_j : number of expectations point in quadrat count to- j

m : total number of quadrat

The null hypothesis is rejected if $X_{hitung}^2 > X_{\alpha,df}^2$ with degrees of freedom $df = m - 1$ or $P\text{-value} < \alpha$ [8].

The spatial dependence between points can also be analyzed using the inhomogeneous K-function, which measures the pairwise distances between all distinct point combinations in the point pattern [18]. The estimated function is:

$$\hat{K}_{inhom} = \frac{1}{D^2|W|} \sum_{i=1}^n \sum_{j=1}^n \left\{ \frac{\|u_i - u_j\|}{\hat{p}(u_i)\hat{p}(u_j)} \right\} h_{ij}(u_i; u_j; r) \quad (6)$$

$$D = \frac{1}{|W|} \sum_{i=1}^n \frac{1}{\hat{p}(u_i)}$$

where:

$h_{ij}(u_i; u_j; r)$: edge correction weight

$|W|$: area of the observation window

$\hat{p}(u_i)$: estimated intensity at $p(u_i)$

$\hat{p}(u_j)$: estimated intensity at $p(u_j)$

The estimated K-function $\hat{K}(r)$ can be visualized to assess whether the pattern is regular, independent, or cluster [11] as shown in Figure 2.

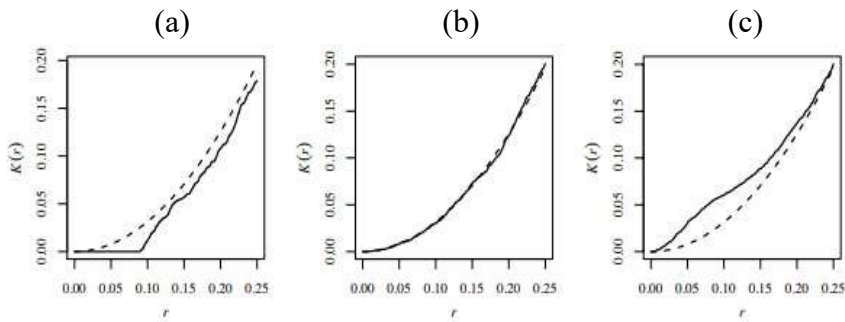


Figure 2. Plot K-Function (a). Regular, (b). Independent (c). Cluster

The illustration in Figure 2 displays a comparison between the empirical K-function $\hat{K}(r)$ and the theoretical K-function under a Poisson process. The dashed line represents the theoretical K-function derived from a homogeneous Poisson process, while the empirical K-function is depicted as a solid line.

Three general patterns can be identified based on the position of the empirical curve relative to the theoretical one. First, when the empirical K-function lies below the theoretical K-function $\hat{K}(r) < K_{pois}(r)$, it indicates that points in the spatial pattern have fewer neighbors than would be expected under complete spatial randomness. This condition suggests a regular or dispersed pattern. Second, when the empirical K-function coincides with the theoretical function $\hat{K}(r) = K_{pois}(r)$, the number of neighbors conforms to what is expected in a purely random distribution, implying a random pattern. Third, when the empirical K-function lies above the theoretical line $\hat{K}(r) > K_{pois}(r)$, it indicates that points have more neighbors than expected under randomness, suggesting a clustered spatial arrangement [21].

Parameter estimation in this study is conducted in two stages. The first stage involves estimating β using the first-order maximum composite likelihood method [11]. The second stage uses second-order composite likelihood to estimate the cluster parameters ω and κ .

This study utilizes secondary data to analyze the spatial characteristics of earthquake events in Eastern Indonesia. The primary response variable is the location of earthquake epicenters, while the explanatory variables include distances from each epicenter to the nearest geological features such as volcanoes, fault lines, and subduction zones. These distances are considered as spatial covariates that may influence the clustering or dispersion patterns of seismic events.

All earthquake data, including coordinates and magnitudes, are sourced from the Indonesian Meteorology, Climatology, and Geophysics Agency (BMKG), the National Earthquake Study Center, and the Center for Volcanology and Geological Hazard Mitigation (PVMBG). To ensure the relevance and severity of the seismic events under study, only earthquakes with magnitudes equal to or greater than 4.5 on the Richter scale are included. The geographic boundaries of the observation window are defined by latitude [6.9264, 4.2063] and longitude [118.5341, 134.9250], covering an estimated area of approximately 100 square kilometers. These parameters provide a focused spatial framework for modeling and prediction. An overview of the spatial variables used in the model is presented in Table 1.

Table 1. Research Variables

No	Variable	Description
1	\mathbf{u}	Coordinates of the earthquake epicenter
2	$Z_1(\mathbf{u})$	Distance to the nearest volcano
3	$Z_2(\mathbf{u})$	Distance to the nearest fault
4	$Z_3(\mathbf{u})$	Distance to the nearest subduction zone

The research procedure follows a systematic workflow designed to capture spatial dependencies and estimate risk using cluster-based spatial point process models. The steps are outlined as follows:

1. Earthquake data for the years 2009 to 2020 were collected from reliable national sources to ensure the validity of the analysis.
2. A data pre-processing step was conducted to filter events based on the defined scope of the study, which includes only seismic events occurring in the Sulawesi and Maluku regions, along with their respective magnitudes.
3. An observation window was defined to specify the spatial boundaries of the study area.
4. The geographic coordinates (latitude and longitude) of earthquake epicenters, as well as the locations of volcanoes, fault lines, and subduction zones, were converted into two-dimensional spatial point pattern objects.
5. Euclidean distances from each earthquake point to the nearest geological feature (volcano, fault, or subduction zone) were calculated to construct covariate variables.
6. Spatial visualization techniques were applied to explore the general characteristics and distribution patterns of earthquake events in Sulawesi and Maluku.
7. An exploratory data analysis was carried out in two stages:
 - a. A chi-square test was applied to examine whether the point pattern exhibited homogeneity (stationarity).
 - b. If the intensity was found to be inhomogeneous, further spatial correlation was explored using the inhomogeneous K-function plot.
8. The inhomogeneous Thomas cluster process was employed to model the spatial distribution of earthquake occurrences in the study area.
9. Model parameters were estimated using first-order and second-order maximum composite likelihood methods.
10. A model validation step was performed using simulation-based envelope plots of the K-function to assess the goodness-of-fit.
11. The validated model was then used to predict the spatial risk of future earthquake events and to produce a risk intensity map for Sulawesi and Maluku.
12. Finally, conclusions were drawn based on the modeling results and prediction outcomes.

3. Results dan Discussion

3.1 Exploration of Earthquake

The analysis commenced with an exploration of the spatial distribution of earthquakes in the Sulawesi and Maluku regions. As illustrated in Figure 3(a), the study focused on seismic events with magnitudes equal to or exceeding 4.5 on the Richter scale. A total of 4,303 earthquake incidents were recorded since 2009 - 2020. These seismic occurrences are depicted as black points, revealing a spatial clustering pattern,

particularly concentrated in the northern and southern regions of Maluku Island. Notably, the majority of earthquakes occurred offshore, while inland seismic activity was relatively infrequent.

To quantify and visualize the distribution pattern more precisely, the study area was divided into a 20×20 unit square grid. As shown in Figure 3(b), each square indicates the number of earthquake occurrences within that specific area. The brighter-colored squares denote higher frequencies of seismic events. The most active grid recorded a total of 166 earthquakes, located in the southern part of Maluku Island. This unit-based representation allows for a clearer understanding of regional earthquake intensity and highlights specific high-risk zones.

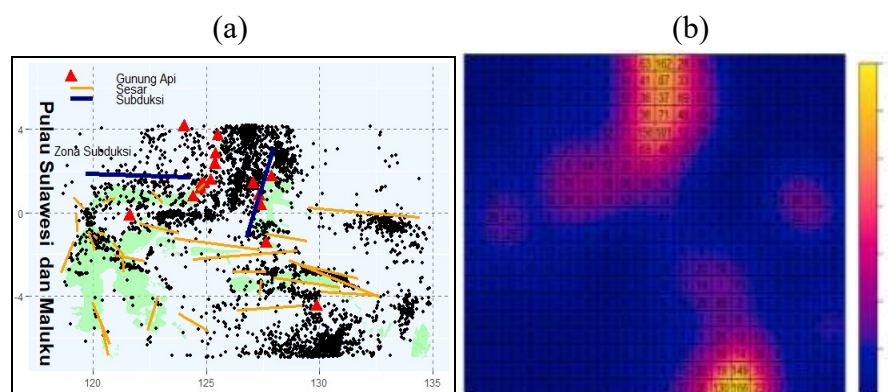


Figure 3. Earthquake Distribution in the Maluku and Sulawesi Regions with Magnitude ≥ 4.5 (a) Earthquake spatial distribution map, (b) Number of earthquake occurrences within each unit square

Based on Figure 3(a), it is evident that the distribution of earthquake occurrences is highly heterogeneous. To statistically validate this observation, a Chi-square test was conducted. The initial step in performing the Chi-square test involved dividing the observation area into 100 grid cells (quadrats), within which the number of earthquake events was counted. This gridded approach facilitates the evaluation of spatial variation in event intensity. The subsequent step involved computing Chi-square test show in Table 2 to determine whether the intensity of earthquake occurrences across the region was homogeneously or heterogeneously distributed.

Table 2. Chi-Square Test

Hypotheses	χ^2	χ^2_{tabel}	<i>P-value</i>	Decision
H_0 : Earthquake intensity in Maluku and Sulawesi is homogeneous	9938.1	123.23	2.2×10^{16}	Reject H_0
H_1 : Earthquake intensity in Maluku and Sulawesi is heterogeneous				

Based on the results presented in Table 2, the computed Chi-square statistic value ($\chi^2 = 9938.1$) is significantly greater than the critical value ($\chi_{tabel}^2 = 123.23$). Therefore, the null hypothesis (H_0), which assumes homogeneous earthquake intensity across the Maluku and Sulawesi regions, is rejected. This leads to the conclusion that earthquake intensity in the study area is spatially heterogeneous. Such heterogeneity may be influenced by geological factors surrounding the region, including the presence of active faults, subduction zones, and volcanoes. Given that the Chi-square test indicates non-homogeneous spatial distribution, it becomes essential to further examine the spatial correlation of earthquake occurrences.

Spatial correlation analysis is conducted to determine whether the pattern of seismic events is regular, independent, or forms clusters. This spatial dependency can be assessed using the inhomogeneous K-function, which provides a statistical measure of clustering in spatial point patterns.

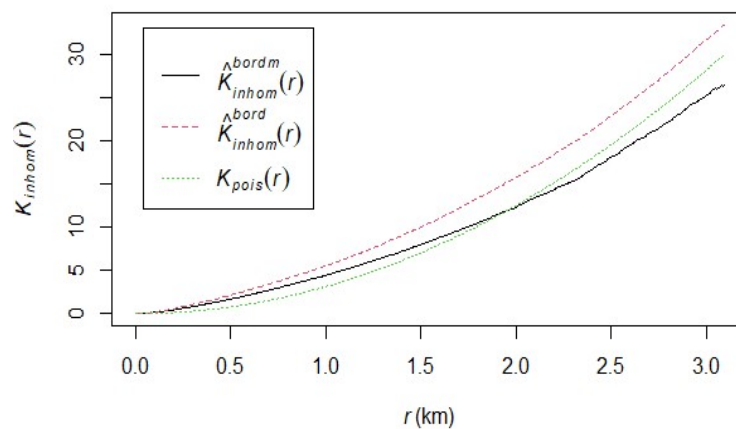


Figure 4. Plot Inhomogeneous K-Function

As shown in Figure 4, the observed K-function with edge correction (represented by the red dashed line) lies above the theoretical K-function for a homogeneous Poisson process (depicted by the green dashed line). This pattern indicates a significant level of spatial clustering in the distribution of earthquake events across the Maluku and Sulawesi. The presence of such clustering suggests that earthquake occurrences are not randomly or independently distributed but instead tend to concentrate in specific locations. Therefore, to appropriately capture and model this spatial dependency, the next step in the analysis involves applying the inhomogeneous Thomas cluster process model, which is suitable for handling non-homogeneous spatial point patterns with clustered structures.

3.2 Inhomogeneous Thomas Cluster Process Modeling

The modeling of the inhomogeneous Thomas cluster process in this study was carried out in two distinct stages. The first stage involved estimating the β parameters, which was accomplished using the Berman-Turner approximation approach. In the second stage, estimation was performed for the κ and ω parameters through the second-order composite

likelihood method. The summary of the estimated parameters β , κ , and ω is presented in Table 3.

Table 3. Estimated Values of β , κ , and ω

Parameter	Estimasi	Exp (Koefisien)	Z-value
	0.5372375		
	0.2570459		
	3.3558007	0.03488	14.0403
	-0.603622	1.82873	-6.4204
	0.3824713	0.68217	3.7554
	0.1543964	0.85693	2.5215

Based on Table 3, it can be concluded that geographical factors specifically, the distances to faults, subduction zones, and volcanoes have a statistically significant influence on the risk of earthquake occurrences. The resulting inhomogeneous Thomas cluster process model is expressed as follows:

$$\hat{\rho}(\mu) = 0.537 \exp(3,356 - 0,604Z_1(u) + 0,382Z_2(u) + 0,154Z_3(u))$$

First, if a location moves 100 km closer to a volcano, the risk of an earthquake increases by approximately 1.8 times. Second, a proximity of 100 km to a fault line raises the earthquake risk by about 0.7 times. Third, when a location is 100 km nearer to a subduction zone, the risk increases by roughly 0.9 times. These interpretations highlight the significant influence of geological factors on earthquake risk.

Furthermore, the clustering behavior of earthquake occurrences is represented by the estimated parameters $\hat{\kappa}$ and $\hat{\omega}$. The estimated value of $\hat{\kappa}$ is 0.5372375, and with a defined observation window area of 224.829 square kilometers, the expected number of primary earthquake events in the Sulawesi and Maluku regions is approximately 121. In addition, $\hat{\omega}$ is estimated at 0.2570459 or 25.70 kilometers, which indicates the standard deviation of the spatial distribution of the largest aftershocks surrounding each mainshock epicenter.

3.3 Goodness Model

Once the earthquake risk model for the Maluku and Sulawesi regions was constructed, model validation was carried out to evaluate its effectiveness in representing the intensity of seismic activity in the study area. This validation step employed the envelope K-function method, which compares the empirical K-function derived from the actual earthquake data with the simulated K-function produced by the inhomogeneous Thomas cluster process model.

To ensure robustness, a total of 99 simulations were performed. This number of iterations was selected based on prior trials indicating that increasing the number of

simulations tends to produce a wider confidence envelope, which improves the reliability of the visual assessment. The resulting envelope plot, which incorporates covariates such as distances to active faults, volcanoes, and subduction zones, is presented in Figure 5.

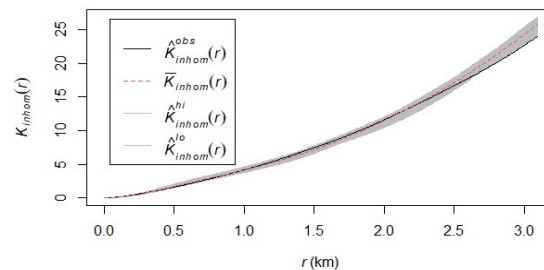


Figure 5. Envelope K-Function Model Inhomogeneous Thomas Cluster Process

As illustrated in Figure 5, the observed K-function (represented by the black line) lies within the simulated envelope bounds, indicating that the inhomogeneous Thomas cluster process model provides a satisfactory fit for modeling the spatial distribution of earthquake events in the Maluku and Sulawesi regions.

3.4 Earthquake Risk Prediction

Following the model evaluation, the next phase involved predicting earthquake risk in the Maluku and Sulawesi regions. This predictive analysis aimed to identify which specific areas are more susceptible to future seismic activity.

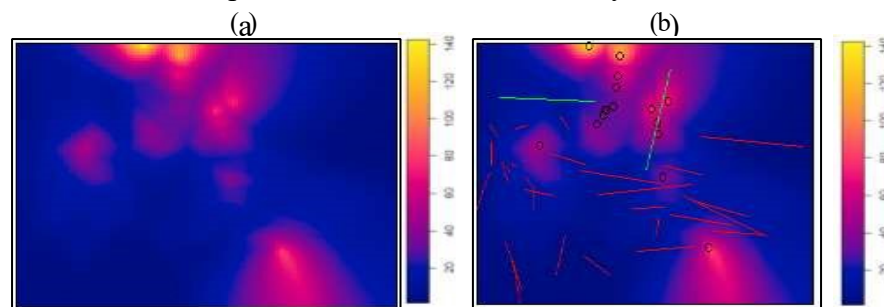


Figure 6. (a) Predicted intensity plot of earthquake occurrences in the Maluku and Sulawesi regions. (b) Predicted intensity plot overlaid with the spatial locations of geological features, including volcanoes, fault lines, and subduction zones.

Based on Figure 6, it can be observed that Sulawesi Island and its surrounding regions are categorized as high-risk zones for earthquake occurrences. This elevated risk is primarily due to the presence of 28 active fault lines, 2 subduction zones, and 16 volcanoes in the area. Detailed risk classification results obtained through the inhomogeneous Thomas cluster process modeling are presented in Table 4.

Table 4. Earthquake Risk Prediction

No	Province	Risk Level
1	Gorontalo	High Risk
2	Sulawesi Utara	High Risk
3	Sulawesi Tengah	High Risk
4	Maluku	High Risk
5	Maluku Utara	High Risk
6	Sulawesi Tenggara	Low Risk
7	Sulawesi Selatan	Low Risk
8	Sulawesi Barat	Low Risk

In reference to the Indonesian earthquake hazard map [20], the provinces of North Sulawesi, Gorontalo, Central Sulawesi, and North Maluku are classified as high risk zones for seismic activity. This is further supported by geological evidence indicating that active faults with depths ranging from 0 to 30 km are concentrated in central to northern Sulawesi and Maluku regions [19]. Moreover, these regions lie at the convergence of multiple tectonic plates, contributing to their elevated earthquake risk levels.

4. Conclusion

The spatial distribution of earthquakes in the Maluku and Sulawesi Islands is characterized by heterogeneity, with seismic events predominantly clustered in northern Sulawesi and southern Maluku. This heterogeneity is statistically supported by the Chi-square test results, which indicate a significant deviation from homogeneity. Furthermore, the observed spatial patterns are influenced by underlying geological factors.

Using the inhomogeneous Thomas cluster process model, this study identified that the intensity of earthquake occurrences in the region is significantly affected by proximity to volcanoes, fault lines, and subduction zones. Specifically, the earthquake risk increases by 1.8 times when a location is 100 km closer to a volcano, by 0.7 times when it is nearer to a fault, and by 0.9 times when it is closer to a subduction zone. Overall, the inhomogeneous Thomas cluster process model demonstrates a strong capacity to accurately model the spatial intensity of seismic events in Maluku and Sulawesi.

The prediction results based on this model indicate that the highest earthquake risk areas are concentrated in northern Sulawesi. High-risk provinces include Gorontalo, North Sulawesi, Central Sulawesi, Maluku, and North Maluku.

References

- [1] Pratiwi, W. R., Asnuddin, Hamdiyah, & Hasriani, S. Pendidikan kespro dalam menghadapi situasi darurat bencana sebagai upaya peningkatan kesejahteraan dan reproduksi sehat. *Indonesian Journal of Community Dedication*, 2(2), 39-44, 2020, <http://jurnal.stikesnh.ac.id/index.php/community/article/view/322>

- [2] Ke, J. P., Labudasari, E., Rochmah, E., & Kunci, K. Literasi bencana di sekolah: Sebagai edukasi untuk meningkatkan pemahaman kebencanaan. *Metodik Didaktik*, 16(1), 41-48, 2020.
- [3] Lubis, M., Simatupang, K. R., & Purwanto, E. Telaah ulang pergerakan lempeng tektonik Indo-Australia dengan menggunakan data GPS tahun 1994–2016. *JoP*, 5(2), 12-16, 2020.
- [4] Sabtaji, A. Statistik kejadian gempa bumi tektonik tiap provinsi di wilayah Indonesia selama 11 tahun pengamatan (2009-2019). *Buletin Meteorologi, Klimatologi, dan Geofisika*, 1(7), 31-46, 2020.
- [5] Pasau, G., & Tanauma, A. Pemodelan sumber gempa di wilayah Sulawesi Utara sebagai upaya mitigasi bencana gempa bumi. *Jurnal Ilmiah Sains*, 11(2), 202-209, 2011, doi:<https://doi.org/10.35799/jis.11.2.2011.208>
- [6] Mardhatillah, E., Anggraini, A., & Nukman, M. Tinjauan perubahan stress Coulomb ko-seismik pada sekuens gempa Palu M 7,5 28 September 2018. *Jurnal Fisika Indonesia*, 24(3), 175, 2020, doi:<https://doi.org/10.22146/jfi.v24i3.58237>
- [7] Trisnisa, F., Metrikasari, R., Rabbanie, R., Sakdiyah, K., & Choiruddin, A. Model inhomogeneous spatial Cox processes untuk pemetaan risiko gempabumi di Pulau Jawa. *Inferensi*, 2(2), 107-111, 2019.
- [8] Baddeley, A., Nair, G., Rakshit, S., McSwiggan, G., & Davies, T. M. Analysing point patterns on networks. *Spatial Statistics*, 42, 100435, 2021, doi:<https://doi.org/10.1016/j.spasta.2020.100435>
- [9] Syaifulloh, A. N., Iriawan, N., & Oktaviana, P. P. Analisis pola persebaran stasiun pengisian bahan bakar umum (SPBU) wilayah Surabaya menggunakan spatial Poisson point process. *Jurnal Sains dan Seni ITS*, 2020, doi:<https://api.semanticscholar.org/CorpusID:213480565>
- [10] Almas, R. Z. Analisis hubungan spasial antara keberadaan pasar modern (minimarket, supermarket, dan hypermarket) dengan toko kelontong di Surabaya menggunakan model marked Poisson point process. *Jurnal Sains dan Seni ITS*, 2020, doi: <https://api.semanticscholar.org/CorpusID:235854729>
- [11] Virania, T. A., Choiruddin, A., & Ratnasari, V. Analisis risiko penyebaran kasus COVID-19 di Surabaya Raya menggunakan model Thomas cluster process. *Inferensi*, 4(1), 57, 2021, doi: <https://doi.org/10.12962/j27213862.v4i1.8874>
- [12] Baddeley, A., & Chang, Y.-M. Robust algorithms for simulating spatial cluster processes. *Journal of Statistical Computation and Simulation*, 1–26, 2023, doi: <https://doi.org/10.1080/00949655.2023.2166045>
- [13] Choiruddin, A., Hannanu, F. F., Mateu, J., & Fitriyanah, V. COVID-19 transmission risk in Surabaya and Sidoarjo: An inhomogeneous marked Poisson point process approach. *Stochastic Environmental Research and Risk Assessment*, 2023, doi: <https://doi.org/10.1007/s00477-023-02393-5>

- [14] Liu, Y., Tian, J., Zheng, W., & Yin, L. Spatial and temporal distribution characteristics of haze and pollution particles in China based on spatial statistics. *Urban Climate*, 41, 101031, 2022, <https://doi.org/10.1016/j.uclim.2021.101031>
- [15] Chiang, W.-H., Liu, X., & Mohler, G. Hawkes process modeling of COVID-19 with mobility leading indicators and spatial covariates. *International Journal of Forecasting*, 38(2), 505–520, 2022, doi: <https://doi.org/10.1016/j.ijforecast.2021.07.001>
- [16] Stindl, T., & Chen, F. Spatiotemporal ETAS model with a renewal main-shock arrival process. *Journal of the Royal Statistical Society: Series C (Applied Statistics)*, 71(5), 1356-1380, 2022, doi:<https://doi.org/10.1111/rssc.12579>
- [17] Böhning, D., Sangnawakij, P., & Holling, H. Estimating risk and rate ratio in rare events meta-analysis with the Mantel-Haenszel estimator and assessing heterogeneity. *International Journal of Biostatistics*, 2022, doi: <https://doi.org/10.1515/ijb-2021-0087>
- [18] Ripley, B. D. Modelling spatial patterns. *Journal of the Royal Statistical Society: Series B (Methodological)*, 39(2), 172-192, 1977, doi: <https://doi.org/10.1111/j.2517-6161.1977.tb01615.x>
- [19] Daryono, M. R. *Paleoseismologi tropis Indonesia (dengan studi kasus di Sesar Sumatra, Sesar Palukoro-Matano, dan Sesar Lembang)*, 2018, doi: <https://api.semanticscholar.org/CorpusID:134660736>
- [20] Pusat Studi Gempa Nasional (Indonesia) & Pusat Penelitian dan Pengembangan Perumahan dan Permukiman (Indonesia). *Peta sumber dan bahaya gempa Indonesia tahun 2017*, 2017.
- [21] Baddeley, A., Rubak, E., & Turner, R. *Spatial point patterns: Methodology and applications with R*. CRC Press, 2015.